Energy and thermal performance evaluation of an automated snow and ice removal system at airports using numerical modeling and field measurements

Article *in* Sustainable Cities and Society · August 2018

DOI: 10.1016/j.scs.2018.08.021

5 authors, including:

S.M. Sajed Sadati
Iowa State University

Kristen Cetin
Michigan State University

Halil Ceylan
Iowa State University

Alireza Sassani
Iowa State University

Sustainable Cities and Society 43 (2018) 238–250

Contents lists available at ScienceDirect

Sustainable Cities and Society

journal homepage: www.elsevier.com/locate/scs

Energy and thermal performance evaluation of an automated snow and ice removal system at airports using numerical modeling and field measurements

S.M. Sajed Sadati[a], Kristen Cetin[b,*], Halil Ceylan[c,d], Alireza Sassani[e], Sunghwan Kim[f]

[a] Research Assistant, Civil, Construction and Environmental Engineering, Intelligent Infrastructure Engineering, Iowa State University, 403 Town Engineering Building, Ames, IA 50011-1066, United States
[b] Assistant Professor, Ph.D., P.E., Civil, Construction and Environmental Engineering, Iowa State University, 428 Town Engineering Building, Ames, IA 50011-1066, United States
[c] Professor, Ph.D., Civil, Construction and Environmental Engineering, ISU Site Director for FAA PEGASAS (Partnership to Enhance General Aviation Safety, Accessibility and Sustainability) Center of Excellence (COE) on General Aviation, United States
[d] Director of Program for Sustainable Pavement Engineering and Research (PROSPER) at Institute for Transportation, 410 Town Engineering Building, Civil, Construction and Environmental Engineering, Iowa State University, Ames, IA 50011-1066, United States
[e] Research Assistant, Civil, Construction and Environmental Engineering, Iowa State University, 176 Town Engineering Building, Ames, IA 50011-1066, United States
[f] Associate Director of PROSPER at Institute for Transportation, Ph.D., P.E., 24 Town Engineering Building, Civil, Construction and Environmental Engineering, Iowa State University, Ames, IA 50011-1066, United States

ARTICLE INFO

Keywords:
Airport operations electrification
Energy management
Power demand
Electrically conductive concrete
Heated pavement
Snow and ice removal

ABSTRACT

Airports are moving toward utilizing clean energy technologies along with the implementation of practices that reduce local emissions. This includes replacing fossil fuel-based with electricity-based operations. These changes would significantly impact the energy demand profile of airports. Electrically-conductive concrete (ECON) is currently a focus of heated pavement design for replacing conventional snow removal practices. ECON heated pavement systems (HPSs) use electricity to heat the pavement surface. Since experimental studies are resource intensive and ECON HPS performance depends on weather conditions, developing a field data-validated numerical model enables its long term energy performance evaluation. In this research, a finite element (FE) model is developed and experimentally-validated using two proposed model-updating methods for full-scale ECON HPS test slabs constructed at Des Moines International Airport (DSM) in Iowa. The model predicts energy demands and average surface temperatures within 2% and 13% respectively. The estimated power demand ranges from 325 to 460 W/m^2 for different weather conditions. The results of this study provide a validated tool that can be used to evaluate the energy demand of ECON HPS. Studying the energy demand of ECON HPS opens the way for developing control strategies to optimize its energy use which will contribute to developing sustainable communities.

1. Introduction

To meet the requirements of a sustainable development, transportation infrastructure, including airports, is moving toward the use of clean energy technologies and reducing the need for conventional practices that create local sources of pollution and have high environmental impacts (ACRP, 2008; Monsalud et al., 2014; Uysal, 2017). This includes replacing fossil fuel-based with electricity-based operations and equipment (Roskilly et al., 2015). However, since the energy demand of such electricity-based operations and equipment would increase the electricity demand profile of the airport, their electric power demand must be assessed to evaluate the technical feasibility of electrifying such operations and equipment. Among the electric systems that could replace conventional practices at an airport, the focus of this research is on electrically-conductive concrete (ECON) heated pavement systems (HPSs) (Anand et al., 2017; Gopalakrishnan et al., 2015a; Gopalakrishnan et al., 2015b).

Snow and ice removal is a necessary effort at many airports, particularly those located in cold regions with frequent and periodic snow and ice events during the winter season. Current methods for snow and

* Corresponding author.
E-mail addresses: ssadati@iastate.edu (S.M.S. Sadati), kcetin@iastate.edu (K. Cetin), hceylan@iastate.edu (H. Ceylan), asassani@iastate.edu (A. Sassani), sunghwan@iastate.edu (S. Kim).

https://doi.org/10.1016/j.scs.2018.08.021
Received 30 May 2018; Received in revised form 31 July 2018; Accepted 15 August 2018
Available online 18 August 2018

Energy and Thermal Performance Evaluation of an Automated Snow and Ice Removal System at Airports Using Numerical Modeling and Field Measurements

S.M. Sajed Sadati[a], Kristen Cetin[b,*], Halil Ceylan[c,d], Alireza Sassani[e], Sunghwan Kim[f]

[a] *Research Assistant, Civil, Construction and Environmental Engineering, Intelligent Infrastructure Engineering, Iowa State University, 403 Town Engineering Building, Ames, IA 50011-1066, United States*
[b] *Assistant Professor, Ph.D., P.E., Civil, Construction and Environmental Engineering, Iowa State University, 428 Town Engineering Building, Ames, IA 50011-1066, United States*
[c] *Professor, Ph.D., Civil, Construction and Environmental Engineering, ISU Site Director for FAA PEGASAS (Partnership to Enhance General Aviation Safety, Accessibility and Sustainability) Center of Excellence (COE) on General Aviation, United States*
[d] *Director of Program for Sustainable Pavement Engineering and Research (PROSPER) at Institute for Transportation, 410 Town Engineering Building, Civil, Construction and Environmental Engineering, Iowa State University, Ames, IA 50011-1066, United States*
[e] *Research Assistant, Civil, Construction and Environmental Engineering, Iowa State University, 176 Town Engineering Building, Ames, IA 50011-1066, United States*
[f] *Associate Director of PROSPER at Institute for Transportation, Ph.D., P.E., 24 Town Engineering Building, Civil, Construction and Environmental Engineering, Iowa State University, Ames, IA 50011-1066, United States*

ABSTRACT

Airports are moving toward utilizing clean energy technologies along with the implementation of practices that reduce local emissions. This includes replacing fossil fuel-based with electricity-based operations. These changes would significantly impact the energy demand profile of airports. Electrically-conductive concrete (ECON) is currently a focus of heated pavement design for replacing conventional snow removal practices. ECON heated pavement systems (HPSs) use electricity to heat the pavement surface. Since experimental studies are resource intensive and ECON HPS performance depends on weather conditions, developing a field data-validated numerical model enables its long term energy performance evaluation. In this research, a finite element (FE) model is developed and experimentally-validated using two proposed model-updating methods for full-scale ECON HPS test slabs constructed at Des Moines International Airport (DSM) in Iowa. The model predicts energy demands and average surface temperatures within 2% and 13% respectively. The estimated power demand ranges from 325 to 460 W/m^2 for different weather conditions. The results of this study provide a validated tool that can be used to evaluate the energy demand of ECON HPS. Studying the energy demand of ECON HPS opens the way for developing control strategies to optimize its energy use which will contribute to developing sustainable communities.

Keywords: *Airport operations electrification, energy management, power demand, electrically conductive concrete, heated pavement, snow and ice removal.*

1. INTRODUCTION

To meet the requirements of a sustainable development, transportation infrastructure, including airports, is moving toward the use of clean energy technologies and reducing the need for conventional practices that create local sources of pollution and have high environmental impacts [1–3]. This includes replacing fossil fuel-based with electricity-based operations and equipment [4]. However, since the energy demand of such electricity-based operations and equipment would increase the electricity demand profile of the airport, their electric power demand must be assessed to evaluate the technical feasibility of electrifying such operations and equipment. Among the electric systems that could replace conventional practices at an airport, the focus of this research is on electrically-conductive concrete (ECON) heated pavement systems (HPSs) [5,6].

Snow and ice removal is a necessary effort at many airports, particularly those located in cold regions with frequent and periodic snow and ice events during the winter season. Current methods for snow and ice removal commonly use fossil fuel-powered vehicles and snow plowing equipment, or melt snow and ice using chemicals [7,8]. During snow removal operations, snow is typically plowed into piles in designated areas [9]. At many airports the piles of plowed snow may also be melted using either stationary or mobile snow-melting equipment. Not only do such conventional methods have high environmental and air quality impacts, they are also time-consuming for airport personnel and can be costly, sometimes resulting in delays and airplane accidents at the airports [10,11]. For this particular type of area, snow and ice can also represent a safety hazard for both passengers and airport workers. Moreover, when chemicals are used for snow and ice removal, the lifetime of the pavement is usually reduced [12,13], resulting in higher maintenance and rehabilitation costs over the pavement's lifetime. Runoff containing such chemicals produce negative environmental consequences [7,14], so there is a growing research focus on alternative snow and ice removal methods, including heated pavement systems [15,16].

Several recent studies have been conducted on heated pavement systems [17–19]. There are four types of heated pavement systems, including: i) infrared heating [20], ii) electrical heaters embedded in pavement [21], iii) hydronic heating circulating hot water through pipes embedded in pavement [22,23], and iv) electrically conductive concrete and asphalt [24–26]. Electrically-conductive concrete (ECON) heated pavement systems (HPS), the most recently developed among these technologies, are produced by adding electrically conductive material, such as steel shavings [26] or carbon fibers [27] to the concrete mix. The addition of these materials enables the pavement system to act as a resistor, which generates heat when a voltage is applied.

ECON HPS require an external source of electricity to generate and dissipate heat that increases the surface temperature of the pavement sufficiently to melt snow and ice. Therefore, the use of ECON HPS will change the profile of electricity demand of an airport during snow and ice events, particularly if it is widely implemented. Given the move toward dynamic and time-of-use pricing by utilities [28,29], as well as the demand charge-dominant rate structures used today, particularly for commercial facilities, a comprehensive understanding of the performance and associated power demands and energy consumption of such systems is needed.

To have an accurate estimation of energy consumption of ECON HPS, it is also necessary to study the thermal performance of this system since the goal of implementing ECON HPS is to use electricity to modulate the pavement surface temperature and melt the snow and ice. ECON HPS's thermal performance depends on many factors, and an important factor is boundary conditions, including climatic conditions, to which the ECON HPS is exposed. Since conducting experimental research to determine thermal performance over a wide range of climatic conditions is costly, the availability of a reliable, validated numerical model for assessing system response under different conditions would be beneficial.

Much of the existing literature on modeling the thermal performance of concrete focuses on the modeling of portland cement concrete (PCC) not containing electrically conductive materials. Thelandersson [30] modeled the combined effects of structural and thermal loads on concrete using coupled equations describing structural and thermal strains. Thermal strain is considered to be a function of concrete temperature and stress level applied by structural loads and a simplified method for estimating the thermomechanical response of concrete to thermal and structural loads was developed and verified by experimental testing.

In another study on material properties of concrete, Khan [31] investigated the significant parameters affecting thermal properties of concrete and models for predicting such properties. Thermo-physical properties of concrete were also studied by Shin, et a. [32] and Kodur and Sultan [33]. In both studies, thermal properties of concrete, including thermal conductivity and heat capacity, were studied for temperatures ranging from 20 to 1,000 ˚C. In this paper temperatures between -20 ˚C and 30 ˚C for concrete material are of interest. The results of Shin and Kodur's studies show that changes in thermal conductivity and heat capacity of concrete are not significant for temperatures between 0 ˚C and 30 ˚C.

In another study, Selvam and Castro [34] developed a 3D finite element model for estimating heat transfer in concrete to seek improvement in its properties for energy storage applications. While this model was used to identify parameters that would improve the performance of concrete in terms of storing thermal energy, these studies have not considered ECON.

Although there are several experimental studies on ECON HPS [18,35], there are only two previously-known studies on numerical modeling of this type of concrete [26,27], and these studies did not consider heat transfer between all pavement layers. Tuan, et al. [26], primarily studied the experimental performance of ECON material produced using steel shavings. A simplified finite element (FE) ECON model was also developed to predict the temperature increase in an ECON layer due to application of a voltage, although the correspondence of the predicted temperature values with experimentally-measured values was not reported. In the second study, Abdualla, et al. [27] developed an FE model of a single ECON layer on top of a regular PCC layer, but did not consider other layers of a pavement system. The ECON material was produced by adding carbon fibers to the concrete mix. Abdualla et al., reported that the temperature values predicted at the middle of the ECON surface by the model were consistent with the laboratory experimental temperature measurements. None of these studies considers the heat loss due to the melting process of snow and ice. Moreover, in previous studies on modeling of ECON, only the top conductive layer has been investigated even though system performance would also be dependent on the heat transfer to the layers below. In addition, in previous studies energy consumption and power demand of the ECON HPS, important factors in operation of these systems, were not evaluated.

Given the non-uniform heating of the ECON layer associated with dispersion of the carbon fibers, along with other complexities of ECON material, a more comprehensive understanding is needed to better characterize the overall performance of ECON, including the associated electricity demand and consumption. This would include modeling of all the pavement layers to produce a more detailed understanding of ECON HPS performance in a physics-based model that can, through validation and model-updating, help predict pavement performance under a variety of conditions in terms of melting snow and ice.

The objective of this research is to create a field data-validated numerical model of ECON HPS capable of predicting its energy demands and temperature variations at multiple surface and sub-surface locations of all pavement layers. This model is developed using actual climatic condition data and system parameters, including material properties and the applied voltage using data obtained from ECON HPS test slabs at the Des Moines International Airport (DSM). Based on this numerical model, the power demand of ECON HPS and resultant effect on the energy consumption of an airport are predicted considering typical weather data for the studied airport location. Although the presented methodology is used to evaluate energy performance of the system at DSM, the methodology can be implemented for any location with available weather data. The methodology of this work are beneficial for providing guidelines for the design of ECON HPS in different climatic zones since the design parameters are highly sensitive to climatic conditions. The effect of implementing ECON HPS on power demand is also an important factor for decision makers who are interested in the feasibility of such systems and comparing them with other snow and ice removal methods. In this respect, having a reliable numerical model that is able to predict the added power demand associated with the use of ECON HPS would be a beneficial tool for developing control strategies to minimize the energy demand. The remainder of this paper provides a brief explanation of ECON material and slab construction, the methodology of obtaining the data from field slabs and developing the FE model, including each layer's material properties and sizing, and model-updating methods for calibrating the model. Results obtained from the model are reported and compared with the actual temperature and electric power measurements under the same climatic conditions.

2. METHODOLOGY

The methodology section is organized into several subsections. The first subsection summarizes the field implementation of ECON, the basis of the developed FE model, including the testing of thermal properties during the field test section. The development of the finite element model is then discussed, followed by a description of the model-updating methods.

2.1 ECON FIELD TESTING

2.1.1 ECON Material

The ECON material was prepared using chopped carbon fibers as an electrically conductive additive. Carbon fiber at a dosage of 1% by total volume of concrete mixture, a value based on the results of previous studies, [5,36–40] was used. The chopped carbon fiber is Polyacrilonitrile-based with 95% carbon content and an electrical resistivity of 1.55×10^{-3} Ω-cm [36]. The carbon fiber fraction of the ECON material mixture, 1% of total volume of ECON, is comprised of 70% 6 mm-long fibers and 30% 3 mm-long fibers.

The ECON mix design [41], materials, and hardened properties conform to standard Federal Aviation Administration (FAA) specifications [42,43]. For the test slabs at DSM, 5 m^3 of ECON material was produced in a drum mixer. Carbon fibers in the required amount were dried in an oven at 115˚C for 24 hours, then packed in water-soluble bags to prevent fiber loss during transportation and handling and to expedite the process of feeding the fibers into the mixer.

2.1.2 Slab Construction and Instrumentation

A full-scale ECON system test slab was constructed at DSM, Iowa [44]. The slab includes a 9 cm ECON layer poured over a 10 cm thick conventional concrete slab with a coarse aggregate base layer of 20 cm underneath, as shown in Figure 1. This pavement design meets the requirements enforced by DSM airport, including having a total concrete layer thickness of 19 cm (in this case

ECON layer (9 cm) plus conventional concrete layer (10 cm)) and base layer of 20 cm. Therefore, ECON HPS can be implemented based on FAA requirements. The ECON HPS consisted of 3.8 m by 4.6 m slabs with six embedded stainless steel L-shaped electrodes spaced 1 m apart. The electrodes were connected to an external source of electricity to provide a voltage of approximately 210 V. Figure 2 is a thermal image of the ECON HPS surface during one of the test events at an average ambient temperature of 0˚C and an average wind speed of 4.1 m/s measured at a height of 10 m.

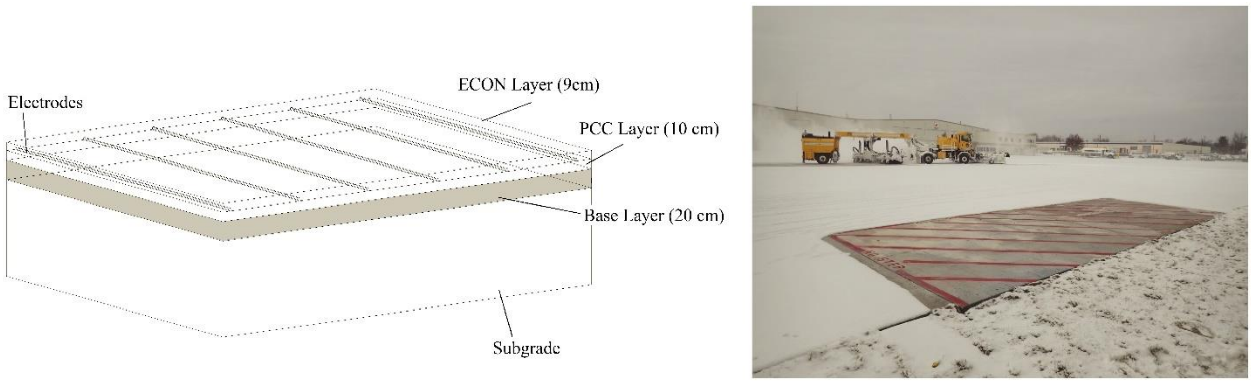

(a) (b)

Figure 1. ECON HPS slabs constructed at the Des Moines International Airport in Iowa, including (a) diagram of the layout and layers, and (b) photograph of the field test setup operating in snow conditions (Photo by Hesham Abdualla, Iowa State University [45]**)**

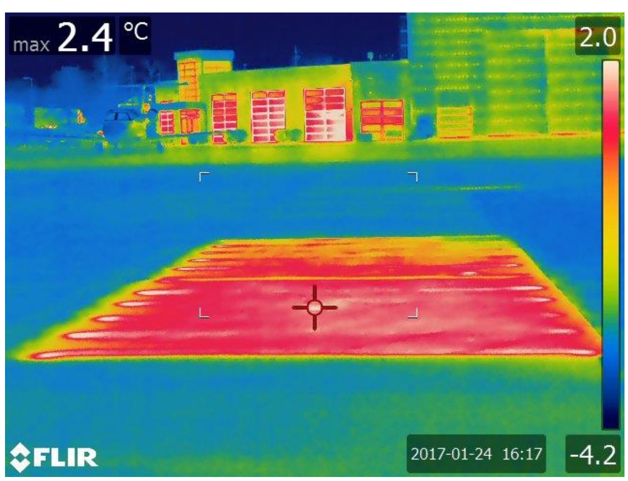

Figure 2. Thermal image of the ECON HPS slabs at DSM in an experimental test under an average ambient temperature of 0 ºC and average wind speed of 4.1 m/s measured at a height of 10 m

2.1.3 Field Data Collection and Quality Control

The field test slabs were implemented with temperature sensors embedded at strategic locations (Figure 2) to provide an improved understanding of thermal performance. The temperature sensors consisted of wireless sensors (with +/- 1% error) [46] and thermistors in installed strain gauge sensors (with +/- 0.5 °C error) [47]. These strain gauges were embedded inside the ECON layer approximately 6 cm from the surface of the pavement, and the wireless sensors were embedded inside each layer of the ECON HPS in the locations shown in Figure 3. The collected field data was quality controlled by checking for sensors and/or periods of time producing noisy data, and for data above or below acceptable temperature thresholds. In order to measure the power demand of the system, voltmeter and ammeter sensors (with +/- 0.5% error) [46] were used on the main circuit connected to the ECON HPS test slabs. Since electric power is the product of voltage and the current values, total error was calculated using multiplication error propagation based on the individual errors of each sensor [48]. The weather data, including ambient temperature and wind speed, were obtained from the US National Centers for Environmental Information [49]. The weather station at DSM is a Class I station, meeting the highest quality standards [50]. The weather condition data used in this study are described in section 2.2.2. Performance data used for model construction and validation in this research, including dates, weather conditions, and snowfall rates and amounts, are summarized in Table 1. As shown in this table, first, Experimental Test 1 measurements are used for performing model updating methodology and calibrating the model then Experimental Test 2 measurements are used as the out of sample data to validate the results of the updated model.

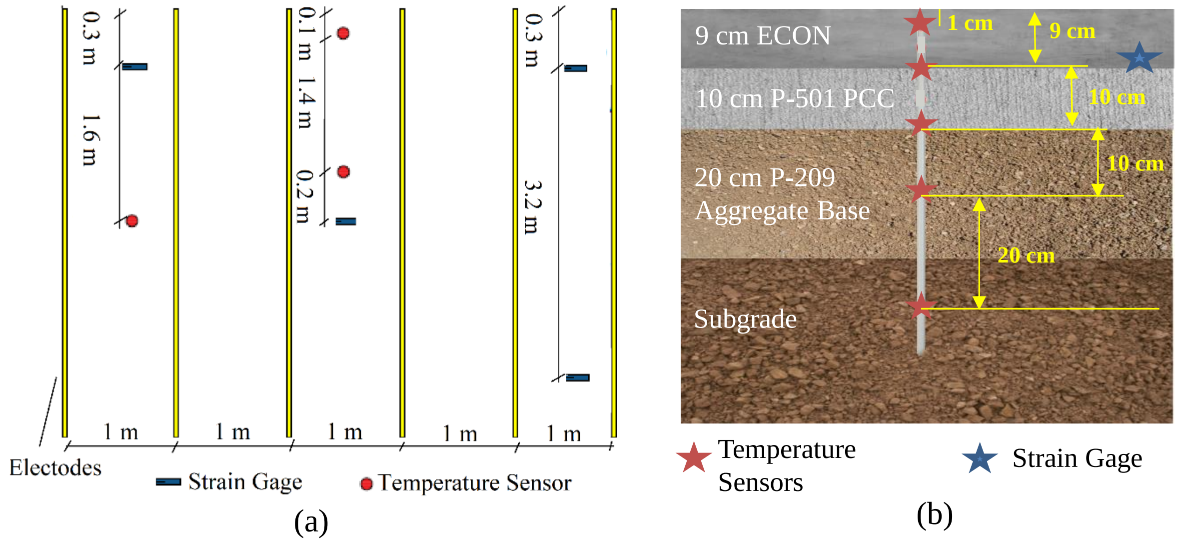

Figure 3. (a) Diagram of sensor layout for field data collection used for finite element model validation, (b) Vertical position of the sensors inside the pavement.

Table 1. Des Moines International Airport field test data summary

Purpose	Operation time (hr)	Avg. Air Temp. (°C)	Avg. Wind Speed (m/s)	Avg. Snow Thickness (mm)	Avg. Power Density (W/m^2)	Total Energy consumption (kWh/m^2)
Experimental Test 1: *Evaluation of FE model with updating*	6	-5	5.8	30	414	2.89
Experimental Test 2: *Evaluation of FE model using out-of-sample data*	2.5	-10	10	12.7	408	0.61

2.1.4 Thermal Properties of ECON HPS Field Test Slab

The physical and thermal properties of the test slabs, including the ECON layer, the conventional concrete layer, the stainless steel electrodes, and the subgrade, are summarized in Table 2. The material properties required for input into the FE model include density, heat capacity, thermal conductivity, and electrical resistivity of each layer.

Thermal conductivity was assessed using a non-contact, non-destructive technique, adapted from a new thermal conductivity measurement method [51], involving a thermal camera and a laser heating element. A focused laser beam was used as a heating element to heat up a chosen area of a bulk sample of the field-implemented ECON. The temperature rise due to the laser beam was used to plot a chart of results of data from materials with known thermal conductivity to determine the thermal conductivity of the field test ECON section. The specific heat capacity was determined by placing the ECON specimen in a foam box filled with water, and using a heat balance equation and measurements of water and concrete temperatures before and after immersion [52]. The electrical resistivity was determined by measuring current and voltage from the constructed slabs at different temperatures [36] and density was measured using samples taken from the concrete layers at DSM during pavement construction. The material properties of the conventional concrete, subgrade and stainless steel electrodes are taken from data available in the literature, including, [27], [53] and [54], respectively. In [53] the thermal properties of subgrade in Minnesota are studied and since the locations are close to Iowa, the same values are assumed for this study. Material properties and possible modifications for better performance of the system, as suggested by Qin [55,56], should be investigated in further studies.

Table 2. Material properties of test slab used for finite element model

Material Type	ECON Slab[1]	Conventional Concrete Layer	Stainless Steel Electrodes[2]	Base Layer[3]	Subgrade[3]
Density (kg/m^3)	2,500	2,300	7,800	1,500	1,500
Heat Capacity (J/kg.°C)	1300	880	475	840	800
Thermal Conductivity (W/m°C)	1.35	1.4	44	1.3	1
Electrical Resistivity (Ω-cm)	900	5.4×10^5	1.7×10^{-9}	5×10^5	1.5×10^4

[1] *Electrical resistivity, heat capacity and thermal conductivity of ECON slab measured at 22 °C*
[2] *Steel properties utilized are based on* [57]
[3] *Subgrade properties utilized are based on* [53]

2.2 ENERGY CONSUMPTION AND POWER DEMAND OF ECON HPS

2.2.1 System Size

It is possible to evaluate the total energy consumption (kWh) and power demand (kW) of the system on either a per-event or a total winter season basis, assuming an ECON HPS constructed as described in sub-section 2.1 are implemented as the sole snow and ice removal method for all typical snow and ice events at DSM. The concrete area where ECON could potentially be located includes the total apron area of DSM, approximately 139,400 m^2. Since it is unlikely that ECON HPS would be implemented to cover the total area of apron, the energy consumption and power demand are calculated based on sizes of four different gate types, to provide a per-gate evaluation. This calculation assumed that 100% of a gate area would be equipped with ECON HPS, as a worst-case scenario, however a smaller portion of the gate area could also feasibly be considered. The approximate required area of apron for each gate type is 2,400 m^2 for Type A, 2,600 m^2 for Type B, 3,000 m^2 for Type C, and 6,500 m^2 for Type D [58]. DSM includes a total of 12 gates, and it is likely that airport managers would want to keep some, if not all, of the gates in operation under winter weather conditions either while it is snowing or after a snowfall. Therefore, providing the results on a per-gate basis can provide decision makers with improved capability for prioritizing ECON HPS operations with respect to highly-used or high-priority gates.

2.2.2 Typical Weather Conditions at DSM

The weather data used to determine the number of snow events and the amount of snow was the Typical Meteorological Year (TMY2) [59] dataset, developed to represent typical conditions in a particular location of interest. TMY3 or TMY4 are not used since snow thickness values are not included in these data sets. TMY2 is based on approximately 20 years of historical weather data for the location of DSM, with hourly increments. Typical snow events were extracted from this data using daily snow thickness, ambient temperature, and wind speed values. For each snow or ice event, the temperature, wind speed, and precipitation rate are applied using the model to calculate the power demand of the system to melt the snow. Since the wind speed data available in TMY are for a height of 10 m above ground level, from those values, wind speed values at 0.5 m above ground level were calculated based on the methodology presented by Sadati, et al. [60].

2.2.3 Energy consumption and System Control Strategy

To determine the energy consumption (kWh) of the total duration of heating, the associated electricity demand profiles are added together at hourly time steps to determine the final energy consumption. To determine the average energy consumption on a per-event basis, the total energy consumption is divided by the number of unique snow or ice events that occurred over the 1 year period of evaluation. Based on the experience of the research team in testing the test slabs of ECON HPS at DSM, since the day of a snow event can be predicted with a higher accuracy than the exact hour of the snowfall within that day, it is assumed that the ECON HPS would operate for the entire 24 hours of the day of a predicted snow event. This assumption is made to simplify the evaluation of energy consumption of the ECON HPS, since typical hourly snow thickness data are not available. Under actual field conditions, based on experimental data, the system could be turned on several hours before onset of predicted snow, such that when snowfall begins the surface temperature would be above the freezing point to prevent snow accumulation. To this end, the control system is given a setpoint as the desired surface temperature and the ECON HPS will automatically turn on whenever the temperature falls below that setpoint. The setpoint in this study is assumed to be 5 °C and the temperature of the surface is checked every half hour.

2.3 FINITE ELEMENT MODEL OF ECON

The ECON FE model, capable of reflecting electrical, thermal, and structural loads and responses is produced in ANSYS 18.2 [61]. ANSYS is commonly used and well-known in the field of thermoelectric FE modeling. To model the thermal performance of the ECON HPS constructed at DSM, transient thermal analysis is used. The elements used for the modeling are the SOLID5 element type for the ECON, PCC, base, and subgrade layers, and the PLANE13 element type for steel electrodes placed within the body of ECON layer. Since SOLID5 and

PLANE13 are capable of handling the electrical, thermal, and structural loads and responses required for the ECON HPS model, more complex element types are not required. These element types are also compatible and can be integrated and used in the same model. There are 9,562 elements in the model, including smaller elements where the mesh size is made finer in and around the electrodes because of their higher aspect ratio. The average size of the elements is approximately 10×10×10 cm^3 for subgrade and as small as 2×2×2 cm^3 for elements close to the electrodes. The meshed model and the elements are shown in Figure 4. The element sizes were found by running the model with the same set of inputs while varying the mesh size and then comparing the results. The change in results was less than 0.5% for element sizes smaller than the selected size. A full transient solution with time-steps of 5 minutes was sought, because this time-step increment provides enough data points for post-processing purposes and is small enough to produce an accurate solution, as checked by running the model using different time-steps.

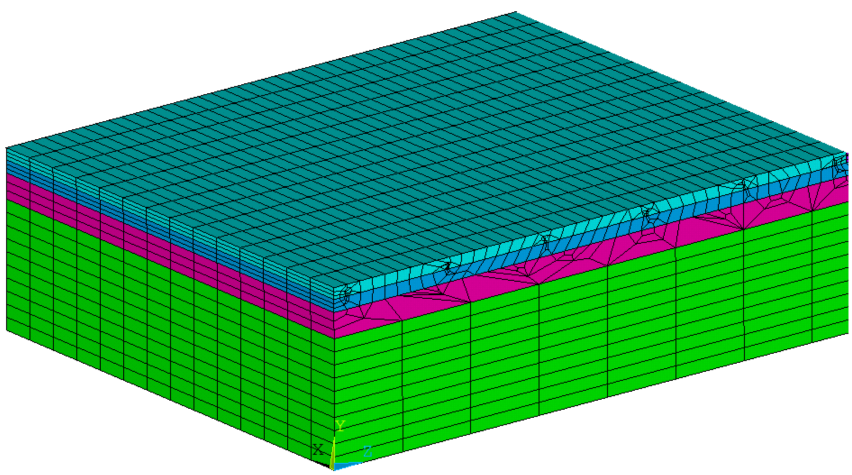

Figure 4. Elements of the finite element model of ECON system

Material properties of the ECON, PCC, base, and subgrade layers, including the density, heat capacity, thermal conductivity and electrical resistivity values given in Table 2, were assigned to the elements.

Heat conduction is assumed to occur between the model layers. Heat loss from the top surface of the ECON layer is modeled as a convection load based on wind speed, because the top surface is assumed to be exposed to outdoor ambient temperature conditions. The convection coefficient is calculated using Eq. (1) [62],

$$h = 4U + 5.6 \quad U < 5m/s$$
$$h = 7.1U^{0.78} \quad U > 5m/s \qquad \textbf{(1)}$$

where, h is the heat transfer coefficient and U is the wind speed. Zero solar radiation is assumed in this model, because the modeling of the slab performance was either for cloudy conditions with minimal diffuse solar radiation or during evening or night hours where there is no solar radiation; the results from this model are thus best applicable for conditions where there are no significant solar loads, which likely to be the case during significant snow events. The vertical sides of the slabs are considered to exhibit negligible heat transfer with surrounding concrete slabs compared to the heat loss from the top surface, an assumption consistent with the modeling methods described in previous literature [27]. Therefore, except for the top surface and heat transfer between interlayers which accounts for the heat loss to the subgrade, the other sides of the model are considered to be adiabatic. The snowfall rate is calculated and a heat flux is applied to the surface of the pavement considering the latent heat required for melting the snow. Sensible heat for increasing the snow temperature from ambient temperature to 0˚C is also applied as a heat flux to the surface of ECON layer. A voltage is applied to each pair of electrodes and the model's heat generation and heat transfer behavior are studied and compared with measured temperature values.

2.4 MODEL-UPDATING METHOD FOR FINITE ELEMENT MODEL

To further improve the model results, updating, also called calibrating, the model to improve the matching of the model results to real-world performance was performed [63]. These resulting modifications involved changes in material properties of the elements used in the model. In this case of a FE model of ECON, the electrical resistivity of concrete depends on its temperature [64], hence the resistivity values of ECON layer samples measured at room temperature (22 °C) may not reflect the actual resistivity of the ECON material in the field. Moreover, while the resistivity of ECON in the FE model is assumed to be homogeneous, it is inhomogeneous in real field applications. The differences between measured resistivity values of samples and the resistivity values of ECON in the full-scale slab are introduced into the FE model using a model-updating method. This model-updating helps to account for assumptions that have been made in the model, including the assumption of homogeneous material properties, which might differ from the actual field conditions. This is done by updating the electrical resistivity value. As a scientific basis for such model-updating, two different parameters are considered: i) temperature of ECON layer, and ii) power demand of ECON HPS. The first is based on the temperatures measured at several points of the ECON layer, while the second is based on the power that could be drawn by the ECON layer. The advantage of considering the second parameter over the first is that it includes the contribution of the whole body of the ECON layer while the first parameter includes temperatures at a few points where the sensors are embedded inside the ECON layer. Making a choice between these two options depends on the modeling objectives, i.e., either estimating the performance of the system in terms of temperature increase, or estimating the energy consumption. These two model-updating methods are explained in the following subsections.

2.4.1 Model-updating Based on Measured Temperature Values

This method uses equations reflective of the conversion of electrical energy to thermal energy and the resulting change in ECON temperature. Eq. (2) calculates the power converted to thermal energy,

$$P = RI^2 \quad \textbf{(2)}$$

where P is the power, R is the resistance of the material, and I is the electrical current flowing in ECON due to the voltage between each electrode pair. R can be calculated using resistivity (ρ) using Eq. (3) [65],

$$R = \frac{\rho L}{A} \quad \textbf{(3)}$$

where, L and A are the length and cross-sectional area of the ECON in the direction of electrical current flow. I can be calculated from the current density (J) by multiplying the electrical conductivity (σ) by electric field (E) as shown in Eqs. (4) and (5) [65].

$$\mathrm{J} = \sigma \mathrm{E} \quad \textbf{(4)}$$

$$|\mathrm{J}| = \frac{I}{A} \quad \textbf{(5)}$$

Temperature increase and thermal energy accumulated inside the slabs can be related using Eq. (6),

$$\frac{dQ}{dt} = mC\frac{\Delta T}{dt} \quad \textbf{(6)}$$

where $\frac{dQ}{dt}$ is the rate of change in thermal energy, m is mass, C is the specific heat capacity, and $\frac{\Delta T}{dt}$ is the rate of change of temperature of the slab. Since it is assumed that electrical energy is the only source of heat generation and there are no other losses, $\frac{dQ}{dt}$ can be set equal to the electric power applied to the slab, as shown in Eq. (7).

$$mC\frac{\Delta T}{dt} = RI^2 \tag{7}$$

Combining Eqs. (4), (5), and (7), and considering that electrical conductivity is the inverse of resistivity ($\sigma = \rho^{-1}$), results in Eq. (8).

$$mC\frac{\Delta T}{dt} = \rho^{-1}\left(\frac{L^2}{A^3}\right)|E|^2 \tag{8}$$

In Eq. (8), the dimensions and material properties (except for resistivity (ρ)) are measureable and do not significantly change with temperature. The resistivity, however, is highly dependent on the temperature of the material. Since the electric field is dependent only on the slab geometry and the applied voltage [65], the resistivity is a good candidate for updating based on measured values in developing an FE model that represents the experimental setup. The temperature increase is proportional to ρ^{-1} and the resistivity value would be updated based on Eqs. (9) and (10), using the measured temperature increase resulting from application of a specific voltage.

$$\frac{\Delta T}{dt} \propto \rho^{-1} \tag{9}$$

$$\frac{\left[\frac{\Delta T}{dt}\right]_{measured}}{\left[\frac{\Delta T}{dt}\right]_{trial}} = \frac{[\rho^{-1}]_{measured}}{[\rho^{-1}]_{trial}} \tag{10}$$

To enable running the simulation to obtain initial results for $\left[\frac{\Delta T}{dt}\right]_{trial}$, trial values of resistivity for a given slab temperature are needed. In this study, this trial resistivity was determined based on the resistivity of ECON samples measured at 22 ˚C and the measured generated current increase in ECON from 0 ˚C to 22 ˚C resulting from the applied voltage.

2.4.2 Model-updating Based on Measured Power Demand

For this method, electric power required by the ECON system can be calculated by the Joule heat generation equation:

$$P = \frac{V^2}{R} \tag{11}$$

where V is the applied voltage. Based on Eq. (10), the power drawn from the energy source is proportional to the inverse of resistance of the system, so the ECON layer resistivity can be updated using Eq. (11), which considers the measured power demand with trial power which is the model estimate.

$$\frac{\rho_{measured}}{\rho_{trial}} = \frac{P_{trial}}{P_{measured}} \tag{12}$$

While model-updating based on power demand would result in a model that is representative of the system in terms of required power, the temperature increase at the surface of the ECON layer should be checked to ensure that the model is also representative of system performance in terms of capability for melting snow and/or ice.

3 RESULTS AND DISCUSSION

The methodology introduced in Section 2 is applied and the results for ECON HPS performance in terms of energy consumption and ability to melt ice and snow in typical climatic conditions of

DSM are reported and discussed in this section. These subsections include the results of the model-updating based on temperature measurements and power demand and the performance of the system under the conditions of typical snow events at DSM.

3.1 MODEL-UPDATING BASED ON AVERAGE TEMPERATURE

Experimental Test 1 data (Table 1), including weather conditions and measured temperature and values are used for the model-updating. The measured resistivity values are used as the trial resistivity values for the model to obtain the initial results and apply the updating method. After model-updating based on the temperature values, the updated resistivity of the ECON layer is calculated. The trial resistivity and updated resistivity values are shown in Figure 5. As shown, the resistivity of ECON decreases with an increase in slab temperature, consistent with the behavior of the resistivity for concrete as reported in the literature [64]. Modifying the resistivity of the model to the updated resistivity values shown in Figure 5, transient thermal analysis is conducted for a simulation time of 5.5 hours, the duration of the Experimental Test 1 in the field.

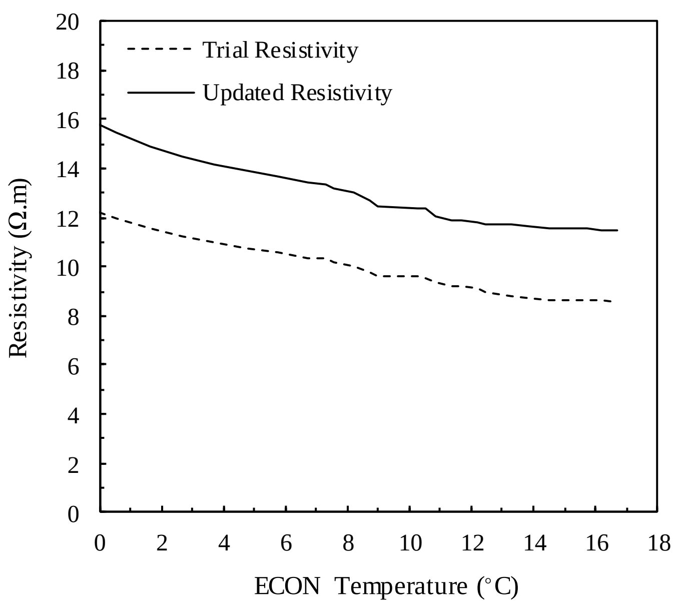

Figure 5. Electrical resistivity of ECON versus temperature for the FE model before and after model-updating by measured temperatures

Figure 6 illustrates the temperature distribution throughout the slab and the heat transfer both to the base layers and to the subgrade. Initial temperatures are assumed for different layers of the pavement based on temperature measurements from sensors embedded in different pavement layers. Since the model is axisymmetric there is no temperature gradient in the direction of the x axis. Although this model is axisymmetric, a 3D model is developed to provide capability in future studies for applying different boundary conditions from the different sides of the slab.

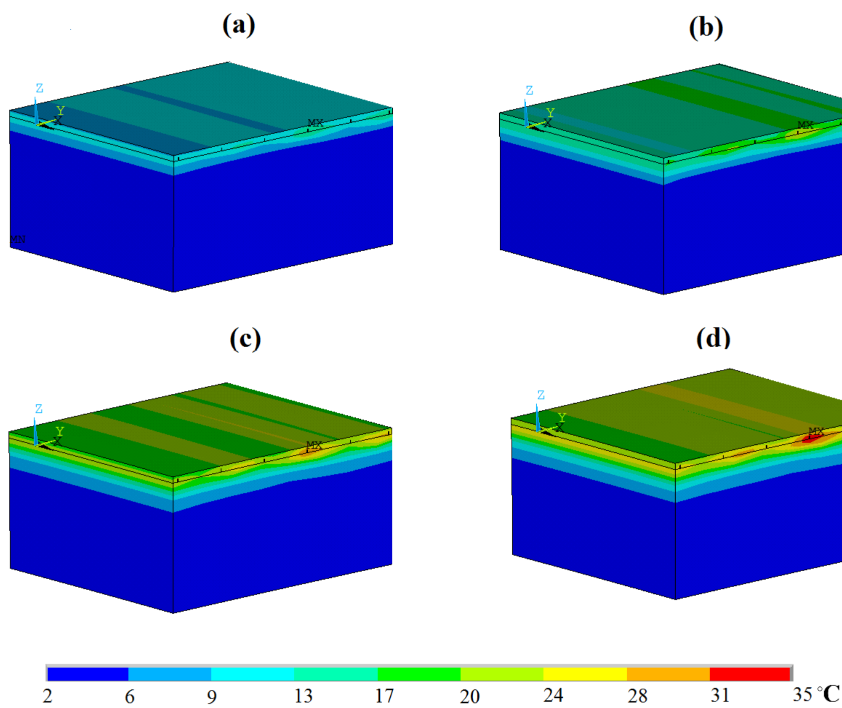

Figure 6. Temperature contours after (a) 1.4 hr, (b) 2.8 hr, (c) 4.2 hr, and (d) 5.5 hr of operation

The average ECON layer temperature resulting from the model and measured in the field are compared in Figure 7. The measurement error bars shown in the figures are calculated based on the potential errors of each sensor. The average ECON layer temperature was measured using the thermistor sensors embedded in this layer. As shown, the FE model results for this test event are consistent with measured temperatures. Therefore, the promising performance potential of the introduced model-updating method can be observed by comparing the non-updated FE and the updated FE model results. The power demand of ECON HPS, both measured at the field and estimated by the updated model based on temperature of the slab, are shown in Figure 8. Although the model-updating method based on measured temperature values aims to improve the estimated thermal performance of the model, it only has a maximum error of 5% in power demand estimation. This updating method can therefore be used for accurately estimating thermal performance and can also provide a close estimation of the power demand.

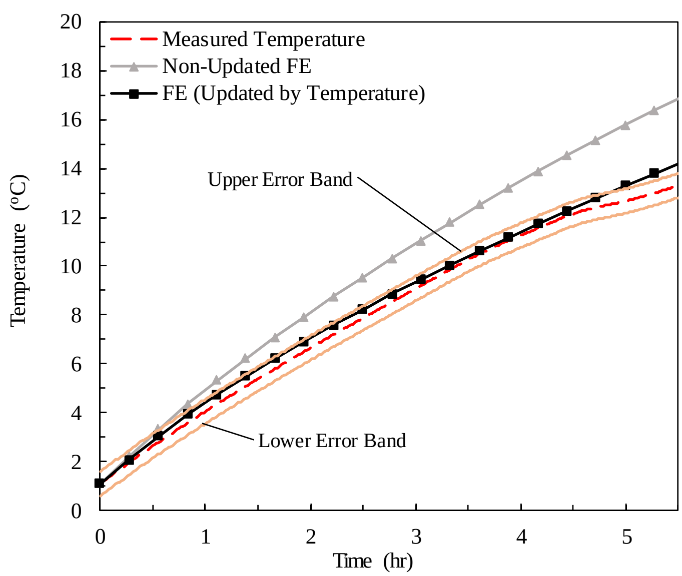

Figure 7. Average temperature of ECON layer for Experimental Test 1 including finite element model simulation results before and after model-updating using measured temperatures (*Note: the average ambient temperature across the test period is -5 °C and average wind speed measured at the height of 10 m is 5.8 m/s; upper and lower error bands present the potential error in measurement calculated using the error value of the temperature sensors*)

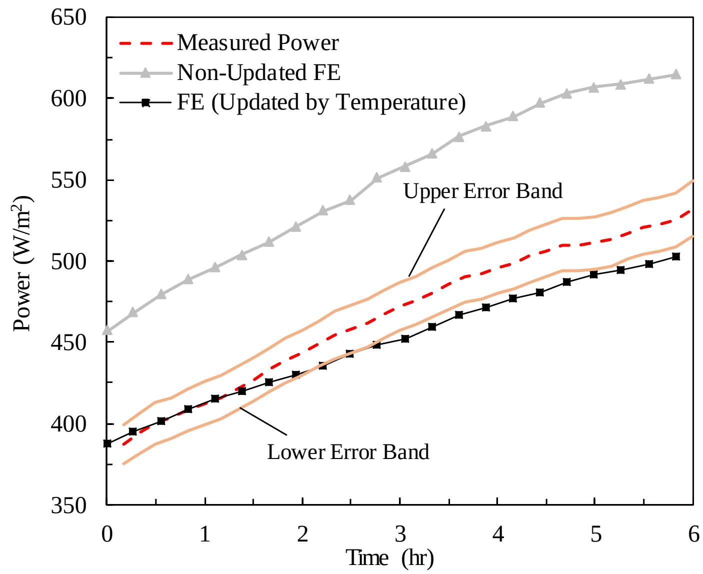

Figure 8. Measured and estimated electric power demand of the ECON HPS for Experimental Test 1 including finite element model simulation results before and after model-updating using measured temperatures ***(Note: the average ambient temperature is -5˚C and average wind speed measured at the height of 10 m is 5.8 m/s during the test period; upper and lower error bands present the measurement error calculated using potential error values for voltage and electric current sensors.)***

To evaluate the performance of the model in weather conditions varying from those used for updating the model, Experimental Test 2 (Table 1), is considered. Figure 9 illustrates the average temperature increase of the ECON layer for Experimental Test 2, reflecting consistency with the measured values and indicating that the model is performing well under different weather conditions and for out-of-sample data.

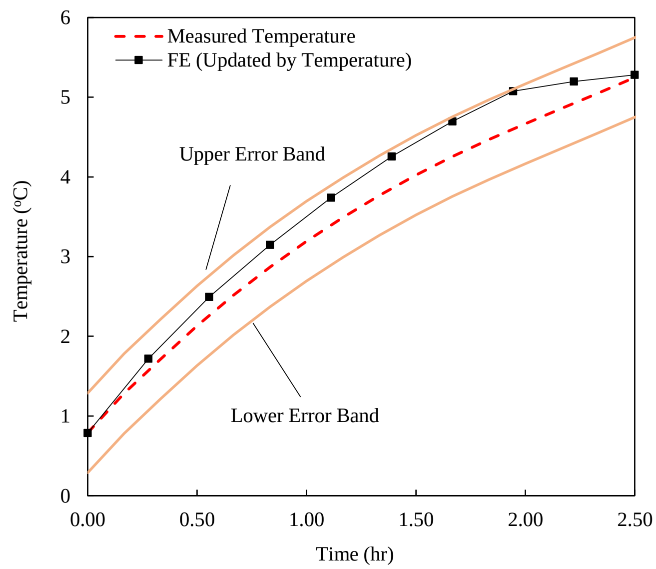

Figure 9. Average temperature of ECON HPS test slab for Experimental Test 2 including finite element model simulation after model-updating using measured temperatures (*Note: the average ambient temperature is -10 ˚C and average wind speed measured at the height of 10 m is 10 m/s; upper and lower error bands present the potential error in measurement calculated using the error value of the temperature sensors)*

3.2 MODEL-UPDATING BASED ON POWER DEMAND

The trial and updated resistivity values obtained by applying model-updating based on power demand and using Experimental Test 1 data are shown in Figure 10. The updated resistivity based on power demand is 16.7% less than the updated resistivity based on the slab temperature and is closer to the measured resistivity (trial resistivity). Measured power and estimated power demand before and after model-updating are shown in Figure 11. Estimating surface temperature for pavements within 5 ˚C error is considered a reasonable accuracy considering complexity of the system [66,67].

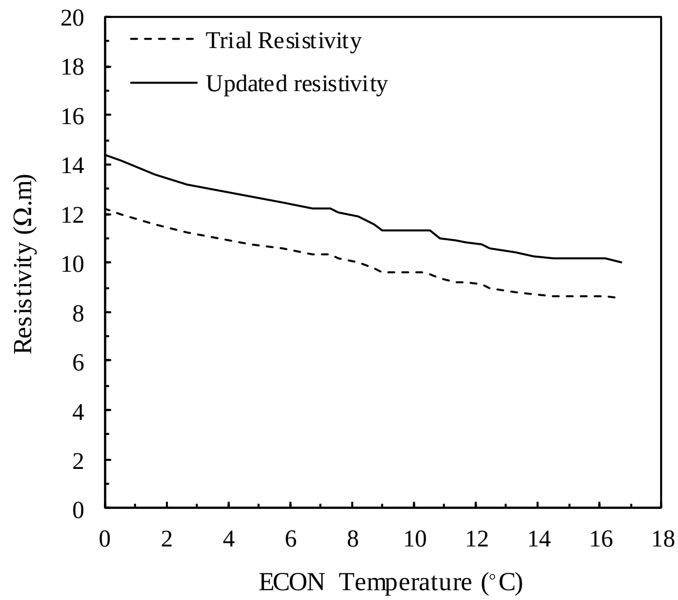

Figure 10. Electrical resistivity of ECON versus its temperature before and after model-updating using measured power demand of ECON HPS

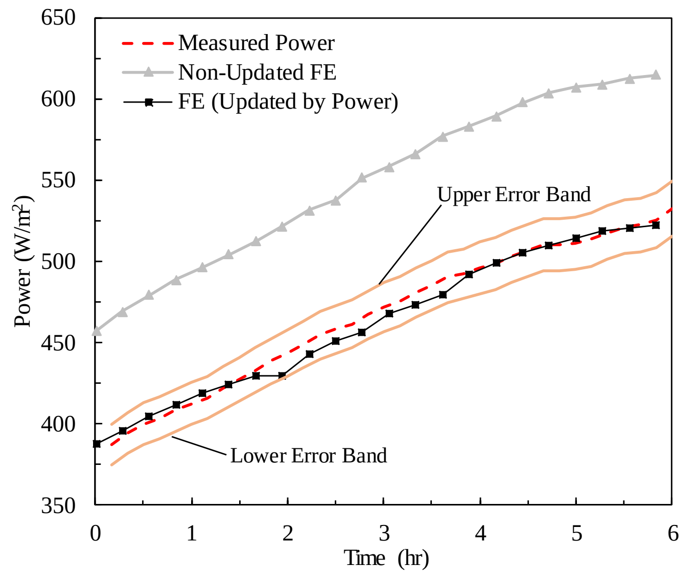

Figure 11. Measured and estimated electric power demand of the ECON HPS for Experimental Test 1 before and after model-updating using measured power demand of ECON HPS (*Note: the average ambient temperature is -5 °C and average wind speed measured at the height of 10 m is 5.8 m/s during the test period; upper and lower error bands present the measurement error calculated using potential error values for voltage and electric current sensors*)

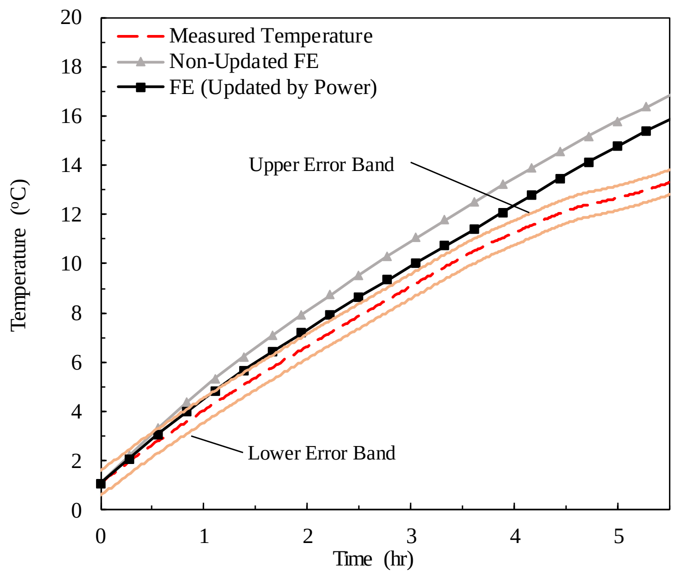

Figure 12. Average temperature of ECON layer for Experimental Test 1 including finite element model simulation results before and after updating using measured power demand of ECON HPS *(Note: the average ambient temperature is -5 °C and average wind speed measured at the height of 10 m is 5.8 m/s during the test period; upper and lower error bands present the potential error in measurement calculated using the error value of the temperature sensors)*

The weather conditions for Experimental Test 2 are applied to the FE model updated by power demand measured for Experimental Test 1 and the estimated electric power demand is shown in Figure 13. As it is shown, the estimated power demand is very close to measured values and this model updated by power is used to evaluate the performance of the system.

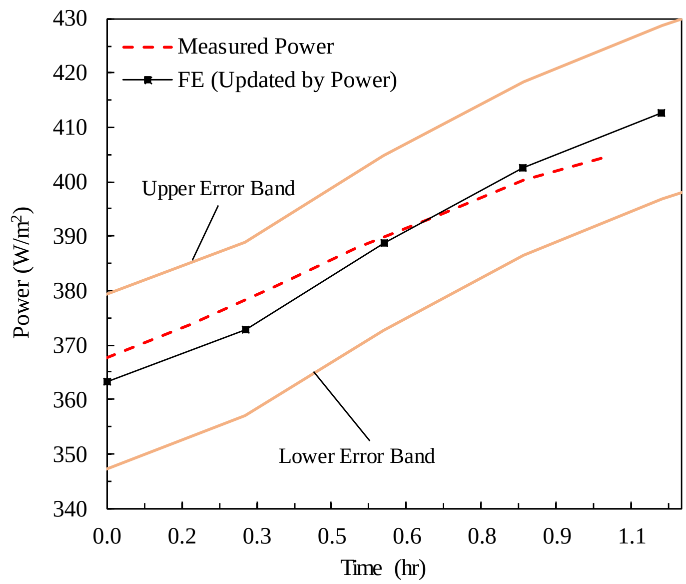

Figure 13. Electric power demand of ECON HPS for Experimental Test 2, including model results after updating using measured power demand of the slab, compared to measured data (*Note: the average ambient temperature is -5 °C and average wind speed measured at the height of*

10 m is 5.8 m/s during the test period; upper and lower error bands present the measurement error calculated using potential error values for voltage and electric current sensors)

3.3 EVALUATION OF ENERGY CONSUMPTION OF ECON SYSTEM

3.3.1 ECON HPS Performance during Typical Snow Events at DSM

The energy consumption of the system under typical snow events at DSM can be evaluated based on the experimentally validated model which was updated using power demand. Hourly ambient temperature, hourly wind speed, and daily snow thickness values were obtained for 32 identified snow events for DSM using the TMY data. These values were applied to the model and the power demand was calculated for each snow event as stated in Figure 14. In order to present details about the process, two examples of these typical snow events which are called event I and event II, are selected to be presented here.

Ambient temperature and wind speed are shown in Figure 15 for snow event I. Average temperature of the ECON HPS surface is shown in Figure 16, where it can be seen that, under these weather conditions, the ECON HPS is able to increase the average surface temperature to the setpoint (5 ˚C) and maintain this temperature. The system turns off and on frequently after it reaches the setpoint temperature so as not to increase the temperature to more than the setpoint value.

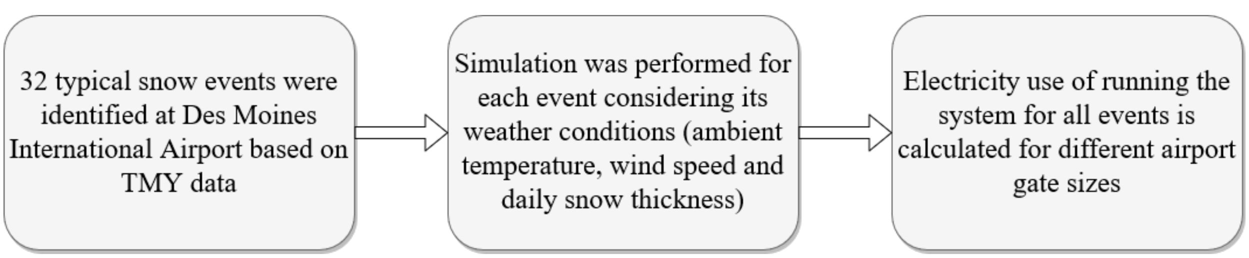

Figure 14. Flow chart of the process for evaluating the electricity use of ECON HPS for a typical winter

Ambient temperature and wind speed values for snow event II are shown in Figure 17. The average temperature of the surface in this case is shown in Figure 18. As can be seen, in extremely cold and windy weather conditions the system was not able to maintain the set point temperature for all hours because of high heat loss from the surface of the slab. Out of 32 typical snow events, however, this is the only one where the designed system is estimated as unable to maintain the surface temperature above the freezing point. In future studies the limitations of the system should be further investigated for these and other extreme weather conditions.

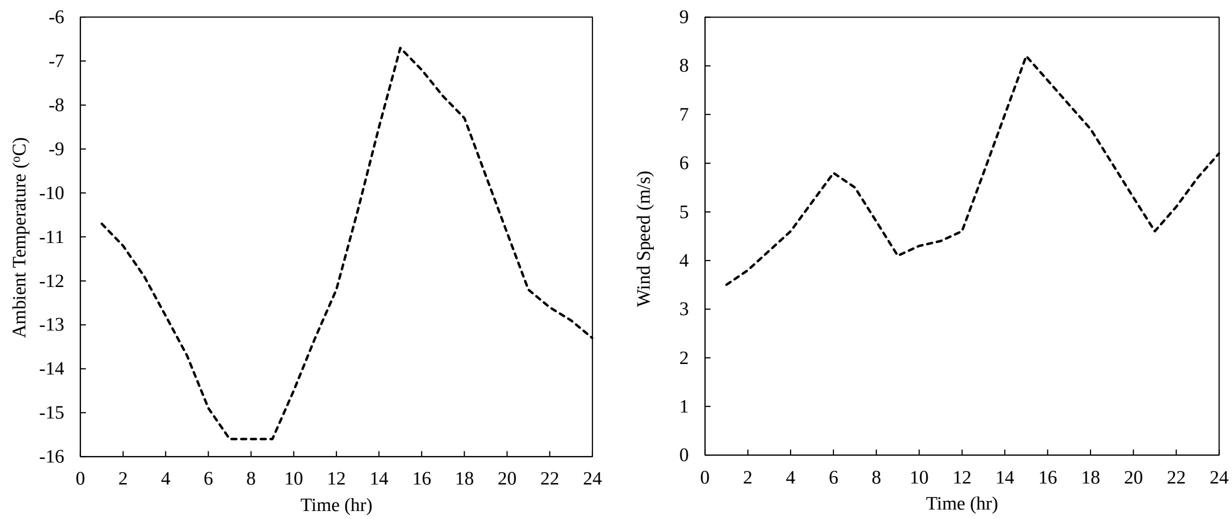

Figure 15. Ambient temperature and wind speed obtained from TMY (typical meteorological year) data for typical snow event I

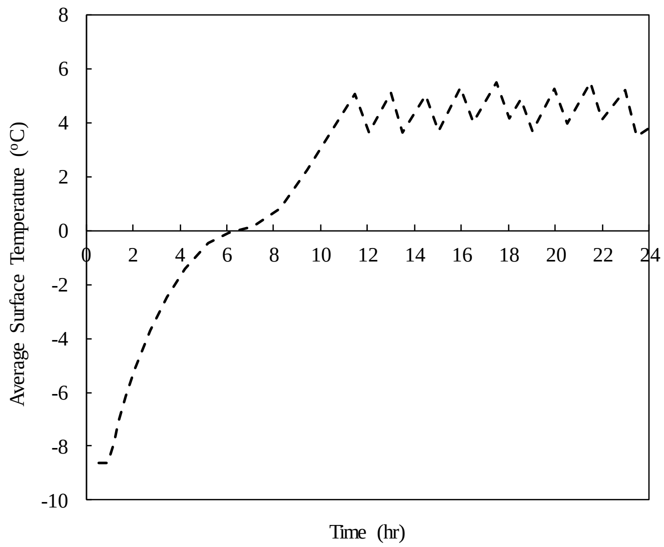

Figure 16. Estimated average surface temperature for ECON HPS for typical snow event I

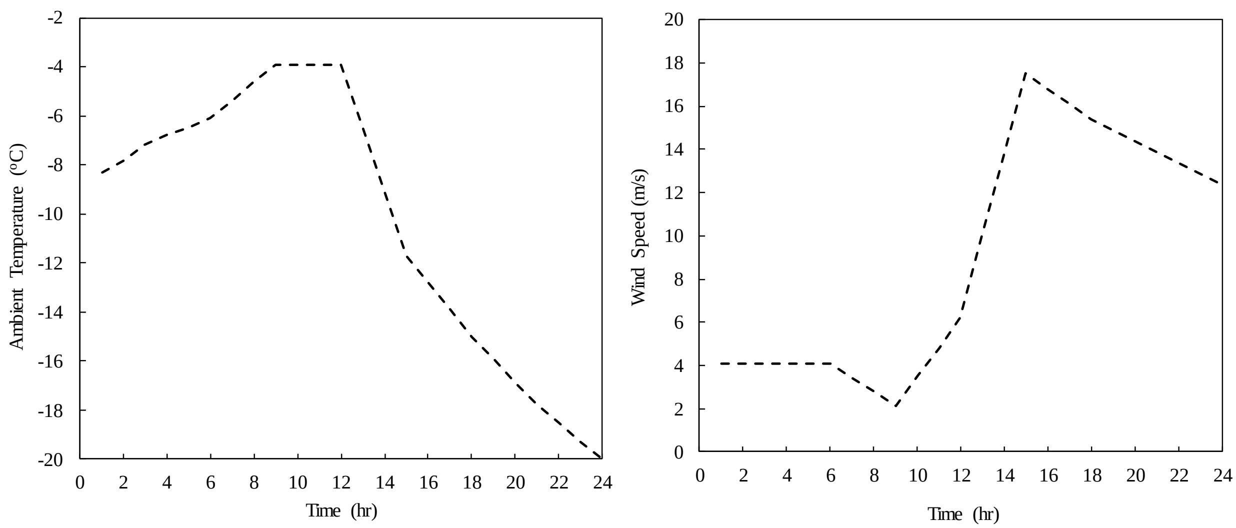

Figure 17. Ambient temperature and wind speed obtained from TMY (typical meteorological year) data for typical snow event II

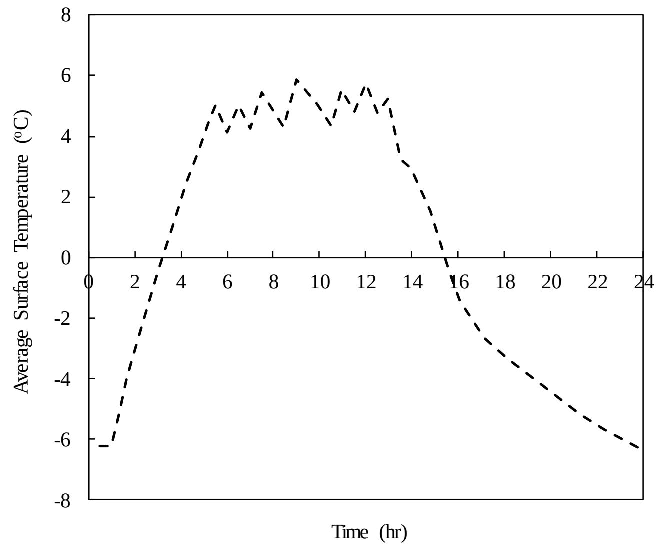

Figure 18. Estimated average surface temperature for ECON HPS for typical snow event II

3.3.2 Power Demand and Energy consumption for ECON HPS

To calculate the power demand, it is assumed that the ECON HPS will be implemented in the gate areas for each gate type introduced in sub-section 2.2.1. The power demand is calculated by running the model using inputs representing the 32 typical snow events. The power demand for the two typical snow events discussed in sub-section 2.1.3 are shown in Figure 19. Due to the higher heat loss from the slab surface in event II which results in lower ECON temperature and higher ECON resistivity, more energy is required if the system is to be able to maintain the setpoint temperature. This higher energy would be provided by decreasing the resistivity of ECON layer and keeping the same applied voltage level. The minimum input energy rate for a hydronic system is reported to be 400 W/m^2 in [68] which is consistent with the values obtained for ECON HPS.

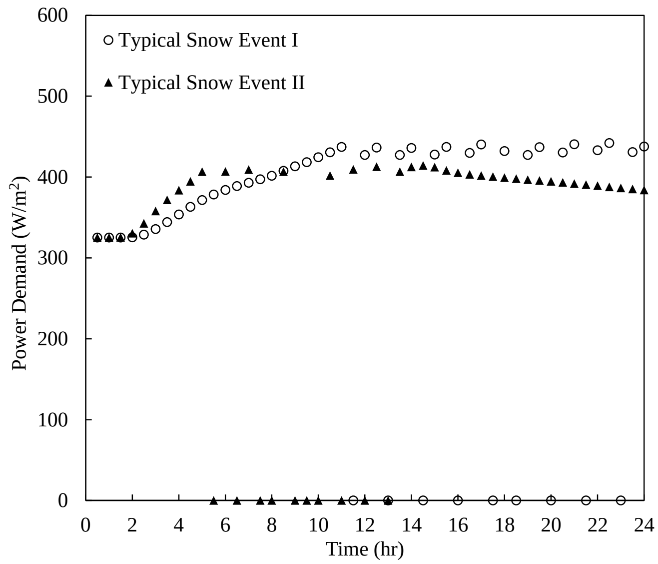

Figure 19. Estimated power demand of the ECON HPS for typical snow events I and II; ***Note: data points for power demand shown at 30 minute intervals; power demand is zero when the system is turned off not to overheat the slab surface***

Considering all the 32 typical events and using power demand calculations from the FE model, the energy consumption is calculated for each gate type. The monthly energy consumption of the system for these gate types for each month of the winter is calculated and compared to the corresponding use at DSM Terminal, a three-story building with 12 gates and an area of approximately 7,000 m^2 , as shown in Figure 20. ECON layer resistivity is the driving factor for the energy consumption of the ECON HPS. Laboratory samples of ECON material exhibited resistivity values approximately ten times lower than those of the ECON material used in the field at DSM. The reason for this difference is the higher efficiency of the mixing procedure in the lab compared to the larger-scale mixing used in the field. It is therefore possible to improve the efficiency of ECON HPS by improving the larger-scale mixing procedure.

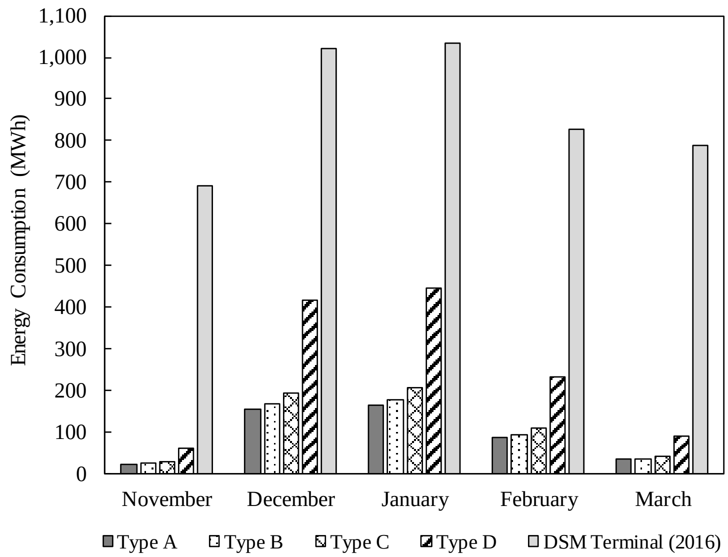

Figure 20. Estimated monthly energy consumption of ECON HPS per gate size for each gate type, considering typical snow events from TMY data in Des Moines, Iowa, in comparison to the measured total monthly energy consumption of the DSM Terminal in 2016

An ECON HPS provides the greatest potential benefit and use for pavements located in cold climate regions, because snow and ice removal is an essential process in these locations [69]. However, even in mixed climate regions that also experience intermittent snow and ice conditions in the winter, critical airport operations may also require substantial snow and ice removal equipment and associated operational budgets [15]. As reported by Anand, et al., [15], in airports with more than 40,000 annual flight operations, critical airport areas should be cleared of snow and ice within a half hour after one inch of snowfall. Satisfying this criteria requires availability of equipment and personnel with an associated high cost of operation, thus mixed climates' airports can also benefit from ECON HPS.

4 CONCLUSIONS

One of the goals of moving toward sustainable transportation is to reduce the emission sources in transportation hubs. Energy demand of electrification of snow removal processes through implementing ECON HPS in an airport was studied in this paper. A FE model was first developed in ANSYS to simulate the performance of ECON HPS test slabs constructed at DSM connected to a 210 V power source, to evaluate the long-term energy demand of this system in large scale. The FE model consisted of all layers of the pavement, including the ECON, PCC, base, and subgrade layers. Methodologies for FE model updating based on measured electric power demand and temperature data were then developed and presented, and the resistivity of the model was updated in order to improve the model results. Updating based on power demand was found to provide more accurate estimation of energy consumption, thus it was used for evaluation of system performance under typical weather conditions for snow events at DSM. The model was programmed to run for all hours of each snow event day and maintain the average surface temperature of the ECON layer at 5 °C. Energy consumption for different types of airport gates was compared to the overall usage of the DSM Terminal. Among 32 typical snow events, in only one case was the system estimated to be unable to keep the surface temperature at the given setpoint due to a very low minimum ambient temperature of -24 °C and a very high maximum wind speed of 18 m/s. In this situations use of conventional snow removal methods might be considered to remove snow and ice. Since hourly typical snowfall data were not available, the analysis was conducted based on daily values of snow thickness, while having data with a higher time resolution would result in more precise modeling. To optimize energy consumption of ECON HPS, the operational gates should be managed in the event of forecasted snow events. ECON layer resistivity is the main driving factor for energy consumption, and improving the large-scale concrete mix techniques could result in saving energy by increasing overall system efficiency. In future studies different strategies for reducing power demand, such as by varying the voltage while the system is running, should also be investigated. Optimal system design in terms of configuration, runoff management and construction processes should also be studied further.

5 ACKNOWLEDGEMENTS

This research was conducted under the Federal Aviation Administration (FAA) Air Transportation Center of Excellence Cooperative Agreement 12-C-GA-ISU for the Partnership to Enhance General Aviation Safety, Accessibility and Sustainability (PEGASAS). The authors would like to thank the current project Technical Monitor, Mr. Benjamin J. Mahaffay, and the former project Technical Monitors, Mr. Jeffrey S. Gagnon (interim), Mr. Donald Barbagallo, and Dr. Charles A. Ishee for their invaluable guidance during this study. The authors also would like to thank PEGASAS Industry Advisory Board members for their valuable support and feedback. The authors would like to thank Mr. Bryan Belt, Director of Engineering at Des Moines International Airport, for his supports throughout this project. Although the FAA has sponsored this project, it neither endorses nor rejects the findings of this research. The presentation of this information is in the interest of invoking comments by the technical community on the results and conclusions of the research.

6 REFERENCES

[1] ACRP, Airport Sustainability Practices, 2008. doi:10.17226/13674.

[2] A. Monsalud, D. Ho, J. Rakas, Greenhouse gas emissions mitigation strategies within the airport sustainability evaluation process, Sustain. Cities Soc. 14 (2014) 414–424. doi:10.1016/j.scs.2014.08.003.

[3] M.P. Uysal, An integrated research for architecture-based energy management in sustainable airports, Energy. 140 (2017) 1387–1397. doi:10.1016/J.ENERGY.2017.05.199.

[4] A.P. Roskilly, R. Palacin, J. Yan, Novel technologies and strategies for clean transport systems, Appl. Energy. 157 (2015) 563–566. doi:10.1016/j.apenergy.2015.09.051.

[5] K. Gopalakrishnan, H. Ceylan, S. Kim, S. Yang, H. Abdualla, Self-heating electrically conductive concrete for pavement deicing: a revisit, in: Transp. Res. Board 94th Annu. Meet., 2015: p. No. 15-4764.

[6] P. Anand, A. Nahvi, H. Ceylan, D. Pyrialakou, K. Gkritza, S. Kim, P.C. Taylor, Energy and Financial Viability of Hydronic Heated Pavement Systems, 2017. doi:DOT/FAA/TC-17/47.

[7] D.M. Ramakrishna, T. Viraraghavan, Environmental impact of chemical deicers--a review, Water. Air. Soil Pollut. 166 (2005) 49–63.

[8] S.M. Quilty, Airside snow removal practices for small airports with limited budgets, 2015.

[9] ACRP, Apron planning and design guidebook, Transportation Research Board, Washington, D.C., 2013. doi:10.17226/22460.

[10] W. Shen, Life cycle assessment of heated airfield pavement system for snow removal, Graduate Thesis and Dessertation, Iowa State University, 2015. doi:Paper 14742.

[11] P. Anand, H. Ceylan, K.N. Gkritza, P.C. Taylor, V.D. Pyrialakou, S. Kim, K. Gopalakrishnan, Establishing parameters for cost comparison of alternative airfield snow removal methodologies, in: The 2014 FAA Worldwide Airport Technology Transfer Conference, August 5-7, 2014, Galloway, New Jersey, 2014.

[12] P. Suraneni, V.J. Azad, O.B. Isgor, W.J. Weiss, Deicing salts and durability of concrete pavements and joints, Concr. Int. 38 (2016) 48–54.

[13] B. Amini, S.S. Tehrani, Simultaneous effects of salted water and water flow on asphalt concrete pavement deterioration under freeze-thaw cycles, Int. J. Pavement Eng. 15 (2014) 383–391.

[14] P.C. Casey, C.W. Alwan, C.F. Kline, G.K. Landgraf, K.R. Linsenmayer, Impacts of using salt and salt brine for roadway deicing, 2014.

[15] P. Anand, H. Ceylan, K. Gkritza, P. Taylor, V.D. Pyrialakou, Cost comparison of alternative airfield snow removal methodologies, (2014).

[16] W. Shen, H. Ceylan, K. Gopalakrishnan, S. Kim, A. Nahvi, Sustainability Assessment of Alternative Snow-Removal Methods for Airport Apron Paved Surfaces, 2017.

[17] J.P. Won, C.K. Kim, S.J. Lee, J.H. Lee, R.W. Kim, Thermal characteristics of a conductive cement-based composite for a snow-melting heated pavement system, Compos. Struct. 118 (2014) 106–111. doi:10.1016/j.compstruct.2014.07.021.

[18] P. Pan, S. Wu, F. Xiao, L. Pang, Y. Xiao, Conductive asphalt concrete: a review on structure design, performance, and practical applications, J. Intell. Mater. Syst. Struct. 26 (2014) 755–769. doi:10.1177/1045389X14530594.

[19] P. Pan, S. Wu, Y. Xiao, G. Liu, A review on hydronic asphalt pavement for energy harvesting and snow melting, Renew. Sustain. Energy Rev. 48 (2015) 624–634. doi:10.1016/j.rser.2015.04.029.

[20] K. Mensah, J.M. Choi, Review of technologies for snow melting systems, J. Mech. Sci. Technol. 29 (2015) 5507–5521.

[21] S.L. Hockersmith, Experimental and computational investigation of snow melting on heated horizontal surfaces, Oklahoma State University, 2002.

[22] C.E. Moon, J.M. Choi, Heating performance characteristics of the ground source heat pump system with energy-piles and energy-slabs, Energy. 81 (2015) 27–32. doi:10.1016/j.energy.2014.10.063.

[23] X. Liu, S.J. Rees, J.D. Spitler, Modeling snow melting on heated pavement surfaces - Part II: Experimental validation, Appl. Therm. Eng. 27 (2007) 1125–1131. doi:10.1016/j.applthermaleng.2006.06.017.

[24] S.M.S. Sadati, K. Cetin, H. Ceylan, Numerical modeling of electrically conductive pavement systems, in: Congr. Tech. Adv. 2017, ASCE, Duluth, MN, 2017: pp. 1–10. doi:10.1061/9780784481011.011.

[25] H. Ceylan, K. Gopalakrishnan, S. Kim, W. Cord, Heated transportation infrastructure systems: existing and emerging technologies, in: The 12th International Symposium on Concrete Roads, September 23-26, 2014, Prague, Czech Republic, 2014.

[26] C.Y. Tuan, Concrete technology today: conductive concrete for bridge deck deicing, Nebraska Department of Roads, 2004.

[27] H. Abdualla, K. Gopalakrishnan, H. Ceylan, S. Kim, M. Mina, P. Taylor, K.S. Cetin, Development of a finite element model for electrically conductive concrete heated pavements, in: the 96th Annual meeting of Transportation Research Board, January 8-12, 2017, Washington, D.C., 2017: pp. 1–18.

[28] P.L. Joskow, C.D. Wolfram, Dynamic pricing of electricity, Am. Econ. Rev. 102 (2012) 381–385.

[29] C. Gu, X. Yan, Z. Yan, F. Li, Dynamic pricing for responsive demand to increase distribution network efficiency, Appl. Energy. 205 (2017) 236–243. doi:10.1016/j.apenergy.2017.07.102.

[30] B.S. Thelandersson, Modelling of combined thermal and mechanical action in concrete, 113 (1987) 893–906.

[31] M.I. Khan, Factors a ecting the thermal properties of concrete and applicability of its prediction models, 37 (2002) 607–614.

[32] K. Shin, S. Kim, J. Kim, M. Chung, Thermo-physical properties and transient heat transfer of concrete at elevated temperatures, 212 (2002) 233–241.

[33] V.K.R. Kodur, M. a. Sultan, Effect of Temperature on Thermal Properties of High-Strength Concrete, J. Mater. Civ. Eng. 15 (2003) 101–107. doi:10.1061/(ASCE)0899-1561(2003)15:2(101).

[34] R.P. Selvam, M. Castro, 3D FEM model to improve the heat transfer in concrete for thermal energy storage in solar power generation, in: ASME 4th International Conference on Ennergy Sustainability, Phoenix, Arizona, 2010: pp. 1–9.

[35] J. Wu, J. Liu, F. Yang, Three-phase composite conductive concrete for pavement deicing, Constr. Build. Mater. 75 (2015) 129–135. doi:10.1016/j.conbuildmat.2014.11.004.

[36] A. Sassani, H. Ceylan, S. Kim, K. Gopalakrishnan, A. Arabzadeh, P.C. Taylor, Influence of mix design variables on engineering properties of carbon fiber-modified electrically conductive concrete, Constr. Build. Mater. 152 (2017) 168–181.

doi:10.1016/j.conbuildmat.2017.06.172.

[37] A. Sassani, H. Ceylan, S. Kim, K. Gopalakrishnan, A. Arabzadeh, P.C. Taylor, Factorial study on electrically conductive concrete mix design for heated pavement systems, in: Transp. Res. Board 96th Annu. Meet., Washington DC, 2017: pp. 17-05347.

[38] H. Abdualla, H. Ceylan, S. Kim, K. Gopalakrishnan, P.C. Taylor, Y. Turkan, System requirements for electrically conductive concrete heated pavements, Transp. Res. Rec. J. Transp. Res. Board. No. 2569 (2016) 70–79.

[39] K. Gopalakrishnan, H. Ceylan, S. Kim, S. Yang, H. Abdualla, Electrically conductive mortar characterization for self-heating airfield concrete pavement mix design, Int. J. Pavement Res. Technol. 8 (2015).

[40] H. Abdualla, H. Ceylan, S. Kim, M. Mina, K. Gopalakrishnan, A. Sassani, P.C. Taylor, K.S. Cetin, Configuration of electrodes for electrically conductive concrete heated pavement, in: ASCE Int. Conf. Highw. Pavements Airf. Technol., n.d.

[41] A. Sassani, H. Ceylan, S. Kim, K. Gopalakrishnan, A. Arabzadeh, P.C. Taylor, Factorial Study on Electrically Conductive Concrete Mix Design for Heated Pavement Systems, in: Transp. Res. Board 96th Annu. Meet., Washington DC, 2017: pp. 17-05347.

[42] FAA, Advisory Circular 150/5370-10G: Standards for specifying construction of airports, 2014. doi:10.1177/004728757301200242.

[43] FAA, Advisory Circular 150/5370-17: Airside use of heated pavement systems, Area. (2005) 1–4. doi:AFS-800 AC 91-97.

[44] U.S. Department of Energy, P. Northwest, Building science-based climate maps, (2013) 2. http://apps1.eere.energy.gov/buildings/publications/pdfs/building_america/4_3a_ba_innov_buildingscienceclimatemaps_011713.pdf.

[45] H. Abdualla, H. Ceylan, S. Kim, M. Mina, K.S. Cetin, P. Taylor, K. Gopalakrishnan, B. Cetin, S. Yang, A. Sassani, others, Design and Construction of the First Full-Scale Electrically Conductive Concrete Heated Airport Pavement System at a US Airport, 2018.

[46] Monnit, Wireless Temperature Sensors, (2017). https://www.monnit.com/Products/Wireless-Sensors/Coin-Cell/Wireless-Temperature-Sensors (accessed December 22, 2017).

[47] Geokon, Vibrating Wire Strain Gage, (2017). http://www.geokon.com/4200-Series (accessed December 22, 2017).

[48] J. Taylor, Introduction to error analysis, the study of uncertainties in physical measurements, 1997.

[49] National Oceeanic and Atmospheric Adminstration (NOAA), National Centers For Environemental Information, (2017).

[50] National Renewable Energy Laboratory (NREL), National Solar Radiation Data Base, (2017).

[51] S. Xu, Optical based thermal probing and characterization, Iowa State University, 2015.

[52] O. Damdelen, C. Georgopoulos, M.C. Limbachiya, Measuring thermal mass of sustainable concrete mixes, J. Civ. Eng. Archit. 8 (2014) 213–220. doi:10.1061/9780784413616.193.

[53] Minessota Department of Transportation, 2007 Minessota DOT Pavement Design Manual, Minessota Dep. Transp. 0 (2007) 1–39.

[54] D. Deng, H. Murakawa, Numerical simulation of temperature field and residual stress in multi-pass welds in stainless steel pipe and comparison with experimental measurements, Comput. Mater. Sci. 37 (2006) 269–277.

[55] Y. Qin, A review on the development of cool pavements to mitigate urban heat island effect, Renew. Sustain. Energy Rev. 52 (2015) 445–459. doi:10.1016/j.rser.2015.07.177.

[56] Y. Qin, Pavement surface maximum temperature increases linearly with solar absorption and reciprocal thermal inertial, Int. J. Heat Mass Transf. 97 (2016) 391–399. doi:10.1016/j.ijheatmasstransfer.2016.02.032.

[57] B. Burgan, N. Baddoo, Structural Design of Stainless Steel, 2012. http://www.bssa.org.uk/cms/File/SCI 291 Structural Design of Stainless Steel.pdf.

[58] FAA, Advisory Circular 150/5360-13: Planning and design guidelines for airport terminal facilities, 1988. http://www.faa.gov/regulations_policies/advisory_circulars/index.cfm/go/document.information/documentID/22618.

[59] National Renewable Energy Laboratory (NREL), Typical Meteorological Year Data, (2000). http://rredc.nrel.gov/solar/old_data/nsrdb/1961-1990/tmy2/ (accessed December 26, 2017).

[60] S.M.S. Sadati, F.U. Qureshi, D. Baker, Energetic and economic performance analyses of photovoltaic, parabolic trough collector and wind energy systems for Multan, Pakistan, Renew. Sustain. Energy Rev. 47 (2015) 844–855. doi:10.1016/j.rser.2015.03.084.

[61] ANSYS Inc., ANSYS®, (2018).

[62] T. Defraeye, B. Blocken, J. Carmeliet, Convective heat transfer coefficients for exterior building surfaces: Existing correlations and CFD modelling, Energy Convers. Manag. 52 (2011) 512–522. doi:10.1016/j.enconman.2010.07.026.

[63] M. Friswell, J.E. Mottershead, Finite element model updating in structural dynamics, Springer Science & Business Media, 2013.

[64] K. Gowers, S. Millard, Measurement of concrete resistivity for assessment of corrosion, ACI Mater. J. (1999) 536–541. doi:10.14359/655.

[65] Z. Xixiang, Z. Benshan, B. Eyjolfsson, Finite element resistivity modelling using specialized mesh structure, National Energy Authority, Reykjavik, Iceland, 1987.

[66] S. Sreedhar, K.P. Biligiri, Development of pavement temperature predictive models using thermophysical properties to assess urban climates in the built environment, Sustain. Cities Soc. 22 (2016) 78–85. doi:10.1016/J.SCS.2016.01.012.

[67] Y. Qin, J.E. Hiller, Ways of formulating wind speed in heat convection significantly influencing pavement temperature prediction, Heat Mass Transf. Und Stoffuebertragung. 49 (2013) 745–752. doi:10.1007/s00231-013-1116-0.

[68] H. Xu, Y. Tan, Modeling and operation strategy of pavement snow melting systems utilizing low-temperature heating fluids, Energy. 80 (2015) 666–676.

doi:10.1016/j.energy.2014.12.022.

[69] A. Nahvi, S.M.S. Sadati, K. Cetin, H. Ceylan, A. Sassani, S. Kim, Towards resilient infrastructure systems for winter weather events: Integrated stochastic economic evaluation of electrically conductive heated airfield pavements, Sustain. Cities Soc. 41 (2018) 195–204. doi:10.1016/j.scs.2018.05.014.